

Comparison of Experimental and Theoretical Determined Terahertz Attenuation in Controlled Rain

Jianjun Ma¹ · Francis Vorrius¹ · Lucas Lamb¹ ·
Lothar Moeller¹ · John F. Federici¹

Received: 21 July 2015 / Accepted: 30 July 2015 /
Published online: 16 August 2015
© Springer Science+Business Media New York 2015

Abstract The effects of rain attenuation on 0.1- to 1-THz frequencies are reported in this paper. The THz pulses propagate through a rain chamber over a 4-m distance and are measured by THz time-domain spectroscopy (THz-TDS). A rain chamber is designed to generate controllable and reproducible rain conditions with different intensities. Image analysis software is employed to characterize the distribution of generated raindrop sizes. Theoretical THz power attenuations due to rain are calculated using Mie scattering theory and are compared with our measurements. Results show that both experimental and theoretical results are in very good agreement with each other.

Terahertz · Wireless communication · Rain attenuation · Mie scattering

1 Introduction

Propagation of terahertz (THz) radiation through the atmosphere is an important consideration for a variety of applications including THz imaging and THz wireless communications. Applications of THz imaging to noninvasive standoff detection of concealed weapons and detecting dangerous materials requires propagation of THz radiation through the atmosphere to the target [1–5]. Atmospheric attenuation of THz radiation also plays a central role in the design and performance of THz wireless communication systems [6–12]. To meet the growing demand for 10–100-Gb/s data rates as predicted by Edholm’s law of bandwidth, the associated wireless carrier frequency will need to be increased into the THz range [6, 7, 13].

For outdoor wireless communications, THz signals can suffer significant impairment because of atmospheric weather conditions [10, 11, 14]. Recent studies have shown how differently THz communication signals are degraded compared to free-space optical signals when passing through the same atmospheric conditions such as fog [15, 16], dust [17], and

✉ Jianjun Ma
jm387@njit.edu

¹ Department of Physics, New Jersey Institute of Technology, 322 King Blvd, Newark, NJ 07102, USA

atmospheric turbulence [18]. Rain attenuation, as another important obstacle to overcome for wireless links and imaging systems with frequencies larger than 10 GHz [19], can lead to an attenuation which degrades THz signal performance. For example, at 103-GHz frequency, a signal suffers 20 dB/km attenuation over a 300-m propagation distance at a 50 mm/h rain rate [20]. So, a suitable rain attenuation prediction method for THz signal performance under rain conditions is required.

There have been many investigations of THz attenuation based on different raindrop size distributions in outdoor rain conditions [21–24]. Several empirical raindrop size distributions have been presented such as exponential distribution, log-normal distribution, gamma distribution, and normalized gamma distribution. In the THz range above 100 GHz, the dependence of the attenuation coefficient A on raindrops can be estimated from [25]

$$A = 4.343 \int Q(D, \nu, n) N(D) dD \quad (1)$$

where $Q(D, \nu, n) = \mu_{th}/N$ is the attenuation cross section as determined by Mie scattering in Eq. (1), n is the refractive index of liquid water, ν stands for the incident frequency, and $N(D)$ represents the drop size distribution as a function of the droplet diameter D . The attenuation A in dB/km is related to the rain rate R and the particular raindrop size distribution model. Hirata et al. accurately predicted the THz attenuation due to rain based on their measurements by using Laws-Parsons model and ITU-specific attenuation model. However, the aforementioned investigated raindrop size distribution models are not suitable for all common rain conditions. In Hirata's study, they also observed an interesting discrepancy between the experimental measurements and predicted theory when comparing the measured BER with attenuation due to rain—as the attenuation increases, the measured BER increases relative to the theoretical predictions from random noise theory used. One possible explanation for the discrepancy between the measured and predicted bit-error-rate in the THz link is wavefront distortions (i.e., scintillations), which will not be included in this work.

Considering the importance of attenuation due to rain for outdoor THz imaging and wireless communications, additional measurements are needed to better understand the frequency dependence of attenuation due to rain in the THz range. However, due to the difficulties in testing wireless links in outdoor weather conditions, such as uncontrollable rain rate, varying raindrop size distributions, and long observation time, it is a great challenge to measure and analyze the impact of weather conditions on THz imaging, sensing, and communications. In our lab, a rain chamber is designed and can realize reproducible and controllable rain conditions under different intensities. Using this rain chamber, the THz attenuation spectrum due to different rain rates can be measured and analyzed by the THz-TDS system.

2 Experimental Setup

The experimental setup consists of a T-Ray 2000™ (Picometrix) Terahertz Time-Domain (THz-TDS) system which transmits and detects broadband THz pulses through artificially generated rain. For this system, the longest path length between the THz transmitter and receiver for normal operation is approximately 1 m corresponding to the length of the rain chamber. In order to create an effectively longer path length, gold mirrors (M1, M2, and M3) are used to reflect the THz radiation multiple times under the rain chamber as shown in Fig. 1a. After the reflection, the total path length through the rain is ~4 m. In order to accommodate the

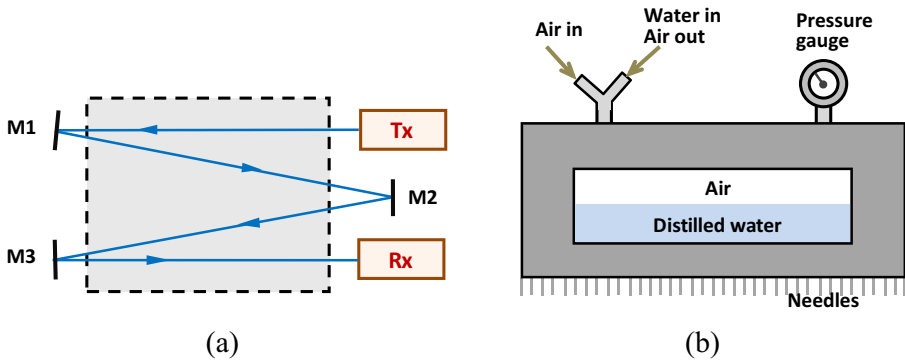


Fig. 1 **a** Illustration of THz beam path in the rain chamber from transmitter (Tx) to receiver (Rx) via reflections from gold plated mirrors (M1, M2, and M3). **b** Side view of the rain chamber. The chamber is constructed from aluminum with a transparent Plexiglas window in the center of the side panel in order to observe the water level while the system is running. Ports on the top of the chamber enable its filling with water, pressurizing the chamber, and monitoring the air pressure inside the chamber. Photo of the rain chamber can be found in [12]

extra time delay in this configuration, the THz waveform which is generated by a femtosecond optical pulse in the transmitter with 2-cm beam diameter is detected by a subsequent optical pulse in the Ti:sapphire laser's pulse train. When collecting THz waveforms for measuring the beam attenuation, the system was set to a rapid scan mode with 1000 averages.

Artificial rain is generated using an enclosed and pressurized chamber, which is filled with distilled water (Fig. 1b). The bottom plate of the rain chamber is machined with 3264 holes in an 8 in. \times 40 in. pattern. Within each hole, a 31-gauge needle is epoxied to produce raindrops. The needles are placed in a cascade pattern so that the rain drops will be uniform across the entire 1-m length of needle array. The diameter of the needles is small enough such that when no air pressure is applied on the water in the tank, no raindrops are produced. This feature enables background scans of the THz transmission to be recorded in the absence of rain. Below the needle array, the water drops fall through a typical distance of 39 cm before they are collected in a shallow plastic bin.

In order to quantify the attenuation of the THz beam due to rain, the rain system must be controllable. This is achieved in the experiment by pressurizing the sealed chamber with air pressure. The air pressure can be fine-tuned when necessary by manually adjusting flow valves while monitoring a pressure gauge. Using this method, it is possible to acquire data at a low rain rate and then incrementally increase the rain rate by increasing the air pressure in the chamber.

To characterize the average rain rate, which is related to the raindrop size distribution, five beakers with an open area of 56.7 cm² are distributed under the rain chamber to collect rain. For a setting time of 60 s, the total volume of water collected in the beakers is measured to calculate the average rain rate. The 1-min averaged rain rate is expressed in units of mm/h to ease comparisons with other scientific reports [26]. Typically, ten measurements of the rainfall are averaged to calculate an average rain rate at a specific pressure. There is a linear relationship between rain rate and pressure as shown in Fig. 2. So, the rain rate can be controllable varied from around 50 to about 500 mm/h by changing the input pressure. Table 1 shows the characteristic of rain intensity with respect to rain rate in millimeters per hour based on World Meteorological Organization (WMO) [27]. Comparing our effective rates

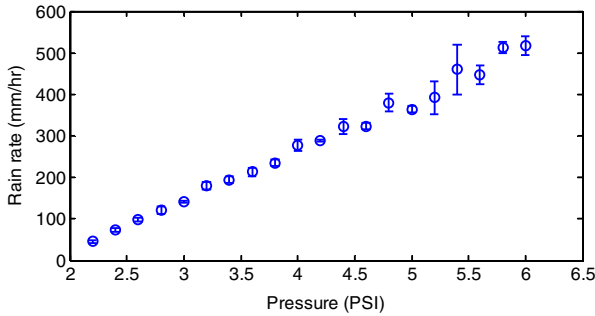


Fig. 2 Rain rate in mm/h from the rain chamber with respect to the air pressure in the chamber. The vertical error bars with 95 % confidence interval shown in the plot represent the standard deviation of recorded rain rates

with those occurring in nature visualizes the feasibility to produce up to heavy rainfalls in our laboratory setup with an effective path length of 4 m.

For the characterization of the size distribution of the raindrops generated from our chamber, pictures of the rain are acquired when the system is running with a constant pressure. In these pictures, individual raindrops are clearly visible relative to a scale which functions as a reference in the measurement of the drop size. It is possible to automatically count the pixels of a raindrop within an image using analysis software (ImageJ) and obtain by this its diameter. Typically 100 drops are measured at each rain rate. It is observed that the size of the raindrops is almost independent of the pressure and rain rate of the chamber. The distribution of raindrop sizes is shown in Fig. 3. In a good approximation, the drop size distribution is approximately follows a Gaussian function with an average diameter of $\bar{D} = 1.9$ mm and a variance of $\sigma^2 = 0.08$ mm².

3 Results and Discussion

3.1 Frequency-Dependent THz Attenuation Through Rain

The THz-TDS waveform through the rain chamber is recorded at a fixed rain rate (fixed air pressure inside the rain chamber), and for each measurement, we determined the rain rate as described in Section 2. As a reference, the THz waveform is also measured in the absence of rain. Using the standard Fourier transform analysis of the time-domain waveforms, the attenuation spectrums of the transmitted THz waveform can be plotted as shown in Fig. 4 for rain rates of 226, 303, and 380 mm/h. The strong peaks at 0.557 and 0.763 THz are caused

Table 1 Rain intensity classification by rain rate [27]

Rain intensity	Rain rate (mm/h)
Light	$R < 2.5$
Moderate	$2.5 \leq R < 10$
Heavy	$10 \leq R < 50$
Extreme	$R \geq 50$

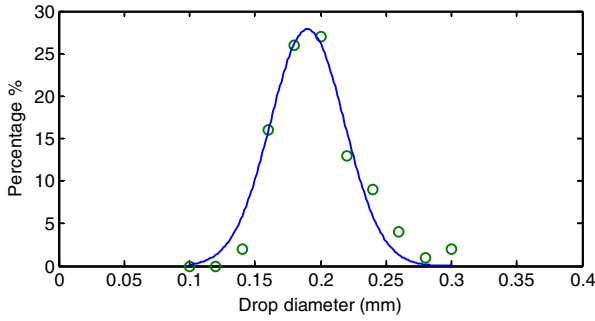


Fig. 3 Measured raindrop size distribution. A Gaussian fit to the data is shown with 1.9-mm average diameter and 0.4-mm distribution width

by water vapor absorptions lines, which is consistent with Grischkowsky’s study [28, 29]. Using the measured attenuation data for different rain rates, the attenuation versus rain rate at a fixed frequency of 625 GHz is plotted in Fig. 5. The relationship between rain rate and attenuation is approximately linear.

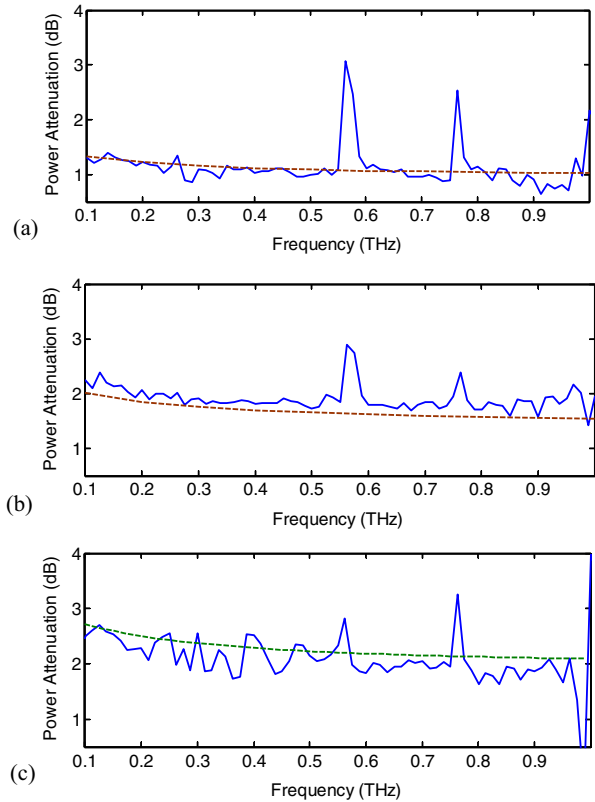


Fig. 4 THz power attenuation spectrum under rain rates of **a** 226 mm/h, **b** 303 mm/h, and **c** 380 mm/h. *Solid and dashed lines* correspond to measured and simulated values, respectively

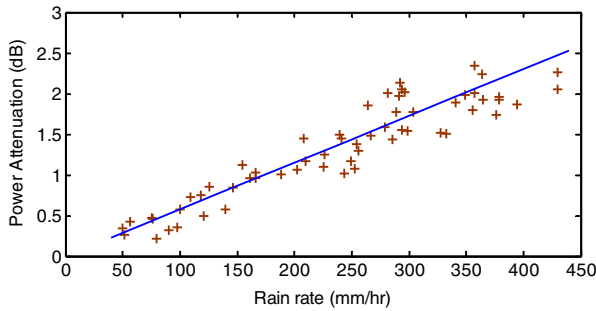


Fig. 5 Measured (*symbols*) and simulated (*solid line*) attenuations of T-rays at 625 GHz for different rain rates

3.2 Predicted THz Attenuation

Simulations of the attenuation can be made assuming that the raindrops act as spherical Mie scattering centers. Following a simple Mie scattering formalism [10, 11, 30], one can estimate the attenuation at THz frequencies based on known raindrop size concentrations. The extinction coefficient takes on the following form:

$$\mu_{th}(\nu) = N \frac{c^2}{2\pi\nu^2} \sum_{m=1}^{\infty} (2m + 1) \text{Re}(a_m + b_m) \tag{2}$$

where N is the number of particles per unit volume, c is the speed of light, ν is the electromagnetic frequency, and a_m and b_m are the coefficients in the infinite summation such that,

$$\begin{cases} a_m = \frac{\psi'_m(y)\psi_m(x) - n\psi_m(y)\psi'_m(x)}{\psi'_m(y)\zeta_m(x) - n\psi_m(y)\zeta'_m(x)} \\ b_m = \frac{n\psi'_m(y)\psi_m(x) - \psi_m(y)\psi'_m(x)}{n\psi'_m(y)\zeta_m(x) - \psi_m(y)\zeta'_m(x)} \end{cases} \quad \text{where} \quad \begin{cases} \psi_m(z) = zj_m(z) \\ \zeta_m(z) = zh_m^{(2)}(z) \end{cases} \tag{3}$$

Here, $j_m(z)$ and $h_m^{(2)}(z)$ are spherical Bessel functions of the first kind and third kind, respectively. The parameter z can be either $x=2\pi\nu r/c$ or $y=2\pi\nu nr/c$, where r is the radius of the spherical particle and $n = \sqrt{\varepsilon}$ is the frequency-independent refractive index of the particle. The relative dielectric constant ε is complex, and its real and imaginary parts refer to the relative permittivity of the raindrop and dielectric loss factor, respectively. This means that there are two main causes of rain attenuation when humidity can be neglected—scattering and absorption effects [31].

For a given rain, the raindrop concentration function can be expressed by using the measured rain rate Rr and raindrop distribution as [32]

$$N(D) = \frac{R}{v_l V_D} \tag{4}$$

Here, V_D refers to the volume of a raindrop with diameter D and v_l stands for the velocity of raindrops inside the laser beam. Then, the THz attenuation in dB/km can be calculated by the integration of Eq. (1) over all the raindrop sizes as shown in Fig. 3.

Figure 4 shows the calculated attenuation as a function of frequency under rain rates of 226, 303, and 380 mm/h based on the Gaussian distribution of raindrop sizes. Theoretical results are compared with the experimental measurements of attenuation due to rain and found to be in good agreement with them. This indicates that the Mie scattering model for spherical raindrops can accurately predict the frequency-dependent attenuation due to rain in the THz range. Furthermore, we conducted a series of measurements under different rain rates. The power attenuation of 625 GHz due to rain is shown in Fig. 5 as a function of the rain rate. In this plot, the experimental and theoretical results are consistent with each other and agree with the results in Fig. 4. This further confirms that our theoretical model is suitable for predicting the THz attenuation in rain weather conditions with different rain rates.

4 Conclusions

Along a beam path of 4-m length THz attenuation due to rain within a frequency band ranging from 0.1 to 1 THz is measured in our lab. A rain chamber is designed which can produce controllable and reproducible rain conditions with rain rates from 50 to 500 mm/h. The THz power loss is measured by using a THz-TDS system when it propagates through the rain chamber. The rain attenuation is simulated by employing a Mie scattering model based on measured Gaussian distribution of raindrop sizes. Calculated results are compared with experiments for a variety of different rain intensities, and results show that they agree well with each other. This confirms that our model can provide a reasonable explanation for obtained experimental data and will enable us to predict the performance of THz wireless communication links in outdoor rainy weather conditions.

Acknowledgments This material is based upon work supported by the National Science Foundation under Grant No. ECCS-1102222. Technical assistance by C. Nicoletti with the THz-TDS instrument is gratefully acknowledged.

Reference

1. I. F. Akyildiz, J. M. Josep and C. Han. "Terahertz band: Next frontier for wireless communications," *Physical Communication*, 12, 16-32 (2014).
2. K. Su, Z. Liu, R. B. Barat, D. E. Gary, Z. H. Michalopoulou, and J. F. Federici. "Two-dimensional interferometric and synthetic aperture imaging with a hybrid terahertz/millimeter wave system," *Applied Optics*, 49, E13-E19 (2010).
3. Z. H. Michalopoulou, S. Mukherjee, Y. L. Hor, K. Su, Z. Liu, R. B. Barat, D. E. Gary, and J. F. Federici. "RDX detection with THz spectroscopy," *J. Infrared Millim. Terahertz Waves*, 31, 1171-1181 (2010).
4. Z. Liu, K. Su, D. E. Gary, J. F. Federici, R. B. Barat, and Z. H. Michalopoulou. "Video-rate terahertz interferometric and synthetic aperture imaging," *Applied Optics*, 48, 3788-3795 (2009).
5. J. F. Federici, B. Schulkin, F. Huang, D. Gary, R. Barat, F. Oliveira, D. Zimdars. "THz imaging and sensing for security applications - Explosives, weapons and drugs," *Semiconductor Science and Technology*, 20, S266-S280 (2005).
6. T. Kürner. "Towards future THz communications systems," *Terahertz Science and Technology*, 5, 11-17 (2012).
7. T. Kürner, S. Priebe. "Towards THz communications-status in research, standardization and regulation," *J. Infrared Millim. Terahertz Waves*, 35, 53-62 (2014).
8. T. Kleine-Ostmann, T. Nagatsuma. "A Review on Terahertz Communications Research," *J. Infrared Millim. Terahertz Waves*, 32, 143-171 (2011).

9. K. R. Jha, G. Singh. "Terahertz planar antennas for future wireless communication: A technical review," *Infrared Physics and Technology*, 60, 71-80 (2013).
10. J. F. Federici, L. Moeller, K. Su. *Terahertz Communication*, in *Handbook of terahertz technology for imaging and sensing*. Woodhead Publishing, Cambridge, 2013.
11. J. F. Federici, L. Moeller. "Review of terahertz and subterahertz wireless communications," *Journal of Applied Physics*, 107, 111101 (2010).
12. J. Ma, F. Vorrius, L. Lamb, L. Moeller, J. F. Federici. "Experimental Comparison of Terahertz and Infrared Signaling in Laboratory-Controlled Rain," *J. Infrared Millim. Terahertz Waves*, 1-10 (2015).
13. S. Cherry. "Edholm's law of bandwidth," *IEEE Spectrum*, 41, 58-60 (2004).
14. Y. Yang, M. Mandehgar, D. Grischkowsky. "THz-TDS Characterization of the Digital Communication Channels of the Atmosphere and the Enabled Applications," *J. Infrared Millim. Terahertz Waves*, 36, 97-129 (2015).
15. K. Su, L. Moeller, R. B. Barat, J. F. Federici. "Experimental comparison of performance degradation from terahertz and infrared wireless links in fog," *J. Opt. Soc. Am. A*, 29,179-184 (2012).
16. Y. Yang, M. Mandehgar, D. R. Grischkowsky. "Broadband THz signals propagate through dense fog," *IEEE Photonics Technology Letters*, 27, 383-386 (2015).
17. K. Su, L. Moeller, R. B. Barat, J. F. Federici. "Experimental comparison of terahertz and infrared data signal attenuation in dust clouds," *J. Opt. Soc. Am. A*, 29, 2360-2366 (2012).
18. J. Ma, L. Moeller, J. F. Federici. "Experimental comparison of Terahertz and Infrared Signaling in a Controlled Atmospheric Turbulence," *J. Infrared Millim. Terahertz Waves*, 35, 1-14 (2014).
19. R. L. Freeman. *Radio System Design for Telecommunications*. Wiley-IEEE Press, New York (2007).
20. T. Utsunomiya, M. Sekine. "Rain attenuation at 103 GHz in millimeter wave ranges," *J. Infrared Millim. Terahertz Waves*, 26, 1651-1660 (2005).
21. S. Ishii, S. Sayama, T. Kamei. "Measurement of Rain Attenuation in Terahertz Wave Range," *Wireless Engineering and Technology*, 2, 119-124 (2011).
22. M. Sekine, S. Ishii, S. I. Hwang, S. Sayama. "Weibull raindrop-size distribution and its application to rain attenuation from 30 GHz to 1000 GHz," *J. Infrared Millim. Terahertz Waves*, 28, 383-392 (2007).
23. T. Utsunomiya, M. Sekine. "Rain attenuation at millimeter and submillimeter wavelengths," *J. Infrared Millim. Terahertz Waves*, 26, 905-920 (2005).
24. A. Hirata, R. Yamaguchi, H. Takahashi, T. Kosugi, K. Murata, N. Kukutsu, Y. Kado. "Effect of rain attenuation for a 10-Gb/s 120-GHz-band millimeter-wave wireless link," *IEEE Transactions on Microwave Theory and Techniques*, 57, 3099-3105 (2009).
25. F. T. Ulaby, D. G. Long. *Microwave Radar and Radiometric Remote Sensing*. University of Michigan Press, Ann Arbor (2014).
26. ITU-R: Specific attenuation model for rain for use in prediction methods. Rec. P.838, ITU-R, (1999).
27. WMO: *Guide to Meteorological Instruments and Methods of Observation*. Geneva, Switzerland (2008).
28. Y. Yang, M. Mandehgar, D. Grischkowsky. "Time domain measurement of the THz refractivity of water vapor," *Optics Express*, 20, 26208-26218 (2012).
29. Y. Yang, M. Mandehgar, D. Grischkowsky. "Determination of the water vapor continuum absorption by THz-TDS and Molecular Response Theory," *Optics Express*, 22, 4388-4403 (2014).
30. C. F. Bohren, D. R. Huffman. *Absorption and Scattering of Light by Small Particles*. Wiley, New York (1983).
31. G. Ivanovs, D. Serdega. "Rain intensity influence on to microwave line payback terms," *Electronics and Electrical Engineering*, 70, 60-64 (2006).
32. M. Khatib. *Contemporary Issues in Wireless Communications*. InTech, Croatia (2014).